sciendo

POLISH MARITIME RESEARCH 2 (126) 2025 Vol. 32; pp. 124-131
10.2478/pomr-2025-0027

Influence of the Plate Dimensions of a Fillet Weld Joint on Angular Deformation and Residual Stresses

Hector Ruíz [1, 2, 3] *
[1] Specialized Superior Technical Institute, Panama City, Panama
[2] National Research System (SNI), SENACYT, Panama City, Panama
[3] Educational Research and Innovation Center in Science and Technology (CiiECYT), Panama City, Panama
Ariadna Sanchez
School of Mechanical Engineering, Technological University of Panama, Panama City, Panama

* Corresponding author: *hruiz@ciiecyt.org.pa (Hector Ruíz)*

ABSTRACT

T-joints are essential structural components in applications such as shipbuilding, where optimised designs are crucial for ensuring load transmission and structural stability. This type of joint exhibits imperfections due to non-uniform heating and cooling behaviour during welding. This study analyses the influence of plate dimensions on the deformations and residual stresses induced by welding on the fillet weld joints. A literature review is conducted to understand the relationship between plate dimensions, angular deformation, and residual stresses, and is followed by a validation study to confirm the simulation methodology. Following this, different models with varying flange widths, plate thicknesses, and web heights are developed using the commercial software MSC PATRAN, and simulations are carried out with the commercial software SIMUFACT WELDING to model the process of gas metal arc welding, using the finite element method. The results confirm the influence of the plate dimensions, revealing that specimens with lower web heights exhibit increased deformation of 15% compared to the average. It is also found that whether the relationship is squared *between the web height and flange width, less angular deformation on the flange will occur. For the plate dimensions and welding conditions considered here, it is found that a thicker flange plate (9 mm) produces greater welding angular deformations than a thinner one (6 mm). This is because depending on the heat input, thinner plates may exhibit less angular deformation than thicker ones when the same amount of heat is applied.*

Keywords: Plate Dimensions, Welding Deformation, Welding Residual Stresses, Finite element Analysis (FEA), T-Joint

INTRODUCTION

In recent decades, the shipbuilding industry has sought to reduce vessel weights by employing thinner steel plates. However, this trend has given rise to challenges in regard to fabrication, in-cluding welding-induced deformations, residual stresses, and crack propagation.

T-joints, a common type of weld, are essential for structural integrity in large-scale steel structures, and are particularly susceptible to these imperfections [1]. Their ability to transmit loads effectively is essential for the overall stability of these structures [2]. However, the residual stresses and de-formations introduced during welding can compromise the performance of T-joints.

These joints are widely used as structural stiffeners, and play a crucial role in transferring loads within a structure [3]. Excessive deformation often occurs, primarily in the vertical plate, during the welding of T-joints [4], and is influenced by factors such as the plate dimensions, the welding speed, and the inherent resistance of the perpendicular plates[1], [5]. In the shipbuilding industry, excessive deformation in stiffeners can lead to misalignments during assembly, thus increasing re-work times and production costs for ship maintenance [1]. In severe cases, accumulated defor-mations can require corrective measures that may introduce additional residual stresses; this is not recommended for this type of joint, which is used to reinforce the hull of the vessel [6]. To mini-mise the deformation, some authors recommend limiting the heat-affected zone to 25% of the plate thickness [6], [7].

Furthermore, the heating and cooling cycles of welding induce residual stresses that are concen-trated in areas sensitive to the process [8]. These residual stresses, combined with deformations, can lead to significant reductions in the strength and premature failure of T-joints [9]. In the con-text of ship construction, residual stresses can affect the product life, particularly under cyclic loading conditions where stress concentration points may become initiation sites for cracks. Under-standing the relationship between plate dimensions and welding-induced deformations is crucial for optimising joint design [10], [11].

Finite element analysis (FEA) represents a powerful tool for simulating welding processes and pre-dicting resulting deformations and stresses [12]. This numerical technique allows engineers to simu-late the welding process in T-joints, enabling them to investigate the resulting deformations and residual stresses within a controlled virtual environment [13], [14].

Current design practices for T-joints often rely on empirical rules or standardised procedures; how-ever, although these methods ensure a base level of structural integrity, they may not account for the specific influence of plate dimensions on the welding process and its effects. This study aims to quantify the relationship between the plate dimensions (thickness, flange width, web height), and the welding-induced deformations and residual stresses in T-joints. We consider realistic weld-ing conditions and validate our results with a referenced case study using S355 steel, which is widely used in the manufacturing of naval structures [15], [16] by carrying out numerical simula-tions using the commercial software MSC PATRAN and SIMUFACT WELDING to support our findings.

REVIEW OF FILLET WELD JOINT VALIDATION

DESCRIPTION OF THE CASE STUDY

A case study involving three identical fillet welded joints specimens manufactured from different steel grades (S355, S700 and S960) was conducted in [1], in which the gas metal arc welding (GMAW) process was implemented. For each specimen, the thickness of the base plate and stiff-ener was 6 mm, while the height of the web was 50 mm. The width and length of the flange were 300 and 130 mm, respectively, as shown in Fig. 1. Sequential welding was carried out in opposite directions: as the welding on one side was finished and the specimen reached ambient room tem-perature, welding on the other side was carried out. The geometry was fully constrained at two nodes on the bottom and top surfaces of the left side, as depicted in Fig. 1. Experimental results such as welding residual stresses and angular distortion are measured. Angular distortion was esti-mated by measuring the vertical displacement of the free edge of the base plate (see Fig. 1).

These authors carried out welding simulations to validate their experimental results[1]. The com-mercial software ANSYS v13 was implemented to carry out a sequentially coupled thermo-mechanical analysis to calculate the residual stresses and distortion of the weld, with the same mesh being used in both the thermal and mechanical analyses. The temperature-dependent thermal material properties of S355 steel grade were obtained using JMat Pro software. The value of the thermal conductivity for S355 is 45 W/m °C at room temperature. Although the heat capacity var-ies strongly with temperature, it does not vary much between different steel grades [1], unlike the thermal conductivity.

A thermal analysis was implemented to evaluate the transient temperature distributions during the welding process. The temperature histories were extracted at points A and B, as shown in Fig. 1, which were located at the mid-section of the fillet welded joint. Point A was located at a distance of 1 mm from the weld toe, while point B was at the centre of the base plate at the bottom. The temperature-dependent yield stress for S355 was approximated by using piece-wise linear equa-tions, while Young's modulus was obtained from [18]. The thermal expansion coefficient was ob-tained using JMat Pro software. Furthermore, the Poisson's ratio was considered to be constant and was set to its value at room temperature (0.29).

During the mechanical analysis, an elastic perfectly plastic material model was considered, as it was assumed that the influence of strain hardening was insignificant. In that study, the influence of solid-state phase transformation steel was not considered. The transverse residual stresses and angular distortion extracted at the top surface of the T-fillet joint's mid-section were compared with experimentally measured values. According to these authors, the numerical predictions showed good qualitative agreement with the experiments.

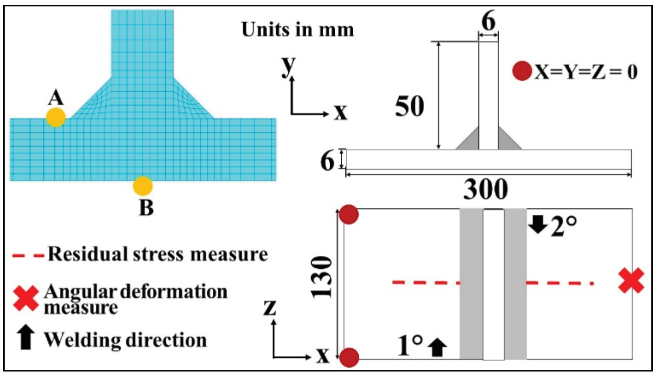

Fig. 1. T-joint geometry: dimensions, boundary conditions, and measurement locations [1]

Tab. 1. Welding conditions for the reference case

Voltage (V)	Current (A)	Welding speed (mm/s)	Leg length (mm)
30	290	8.3	6

COMPARISON WITH THE CASE STUDY

To validate the methodology and material behaviour, a finite element analysis (FEA) is conducted here using the commercial software packages MSC PATRAN[17] and SIMUFACT WELDING [18]. SIMUFACT WELDING allows the user to carry out a coupled thermo-mechanical analysis to calculate the temperature distribution, welding residual stresses and welding distortion. A re-fined hexahedral element is generated, with finer elements near the fillet and progressively coarser elements towards the edges. The reference model was subjected to the same welding conditions and boundary conditions as used in [1], while the material properties of S355 steel were taken from the software's material library [18]. The scheme used to conduct the simulations is shown in Fig. 2.

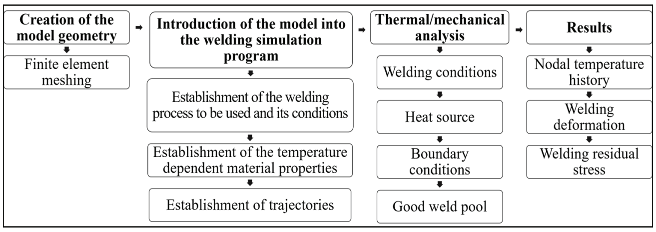

Fig. 2. Scheme for conducting the simulations

Mesh Sensitivity Study

A mesh sensitivity analysis was conducted to assess the impact of element size on the accuracy of the results and the computational efficiency of the welding simulation. Three mesh configurations were considered, as shown in Table 2, along with the simulation time and the average of the differences between them, as follows: M1, with smaller elements in the heat-affected zone (HAZ), gradually increasing in size in the transverse direction; M2, a uniformly fine mesh with elements of the same size throughout the joint; and M3, which also had elements of the same transverse size but varying longitudinally. Variations in angular distortion, temperature distribution, and residual stresses were analysed by comparing the results to a reference value to assess convergence. The results indicated that while M2 provided the highest accuracy, its high computational cost made it impractical for extensive studies. In contrast, M1 yielded acceptable accuracy with a significant reduction in computation time, making it the optimal mesh selection for this study, which priori-tised a balance between numerical fidelity and computational feasibility.

Tab. 2. Mesh configurations

Mesh	Element Size	Time	Desv.
M1	10 × 1 × 1	14 m 56 s	–
M2	1 × 1 × 1	5 h 45 m 55 s	0.034
M3	5 × 1 × 1	1 h 14 m 54 s	0.026

Thermal comparison

A thermal analysis was conducted by comparing the simulated temperature distribution with exper-imental data [1]. Fig. 3 presents temperature histories for points A and B, located at similar posi-tions to those in the simulated and experimental models.

Points A and B exhibit similar temperature profiles with comparable values. Accuracy is estimated at about 98% and 90%, respectively, based on the maximum peak values. This close agreement validates the welding conditions and material properties considered here, and demonstrates their ability to accurately reproduce the experimental thermal behaviour.

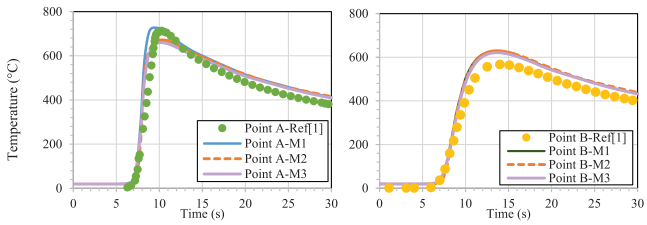

Fig. 3. Comparison of temperature profiles at points A and B (simulations)

Mechanical comparison

A comparison of the simulated and experimental results for the deformation and transverse residu-al stresses was conducted using data from [1]

Fig. 4 shows similar angular deformation patterns, with minimal deformation on the left flange and positive angular deformation on the right-hand plate. A discrepancy of approximately 19% is ob-served between the simulated results and the experimental data presented in [1], which can be at-tributed to potential discrepancies in the mechanical properties of the material, measurement errors, mesh size limitations, and solver specifics.

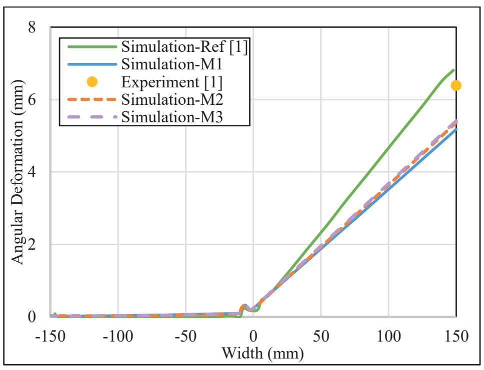

Fig. 4. Comparison of angular distortion at weld centre (simulation vs. case study [1])

Fig. 5 compares the simulated and measured transverse residual stresses across the top surface welding line at the mid-length [1]. This comparison reveals good agreement between the simulated and measured transverse residual stress profiles across the weld line, which validates the accuracy of the simulation procedure in predicting residual stress distribution.

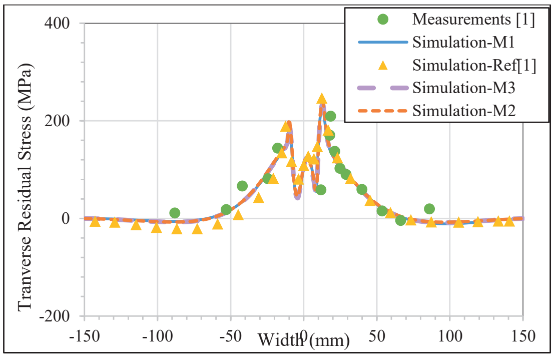

Fig. 5. Comparison of transverse residual stress (simulation and measurement)

NUMERICAL ANALYSIS OF PROPOSED CASES

DESCRIPTION OF PROPOSED CASES

Fourteen finite element models were developed to assess the impact of the width, thickness, and web height on welding-induced angular deformations and residual stresses. When conducting these simulations, the same scheme was implemented as presented in Fig. 2.

For this simulation, T-joint models with a constant flange length of 500 mm and a leg size of 6 × 6 mm were generated. The flange width, web height, and plate thickness varied as outlined in Table 3.

Tab. 3. Proposed models

Model	Cases	Flange			Web	
		Length	Width	Thickness	Height	Thickness
A	A-0	500	500	9	300	9
	A-1		500	9	200	9
	A-2		500	9	100	9
	A-3		500	6	300	6
	A-4		500	6	200	6
	A-5		500	6	100	6
B	B-0		200	9	300	9
	B-1		200	9	100	9
	B-2		200	6	300	6
	B-3		200	6	100	6
C	C-0		300	9	300	9
	C-1		300	9	100	9
	C-2		300	6	300	6
	C-3		300	6	100	6

FINITE ELEMENT MODELS

Finite element models were generated using MSC PATRAN [17], with a hexahedral element with a minimum element size of 10 × 1 × 1 mm being employed around the fillet region to ensure accu-rate stress analysis (Fig. 6). The element size increases progressively away from this critical area. The complexity of the models varied, with model A-0 consisting of 44,982 nodes and 3,600 ele-ments. A perfectly plastic elastic model was used.

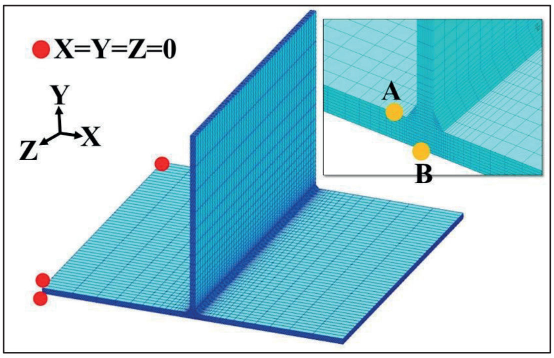

Fig. 6. Fillet weld joint (case A-0)

Material properties and boundary conditions

S355 steel was chosen as the material for the analysis, and its thermo-mechanical properties were retrieved from the software's material library [18]. Fig. 7 shows the thermal-mechanical properties used in this study. The density was considered to be constant at 7,840 kg/m3, and the mechanical boundary conditions were the same as those considered in the comparison with[1] (see Fig. 6).

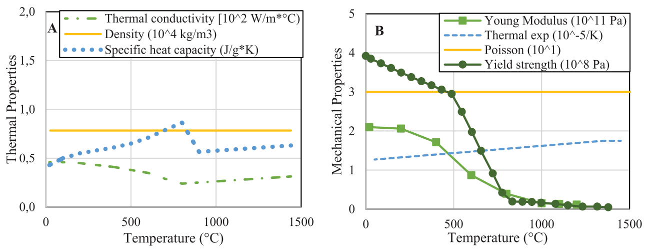

Fig. 7. Material properties: (A) thermal; (B) mechanical

THERMAL ANALYSIS

The GMAW process was simulated using the commercial software SIMUFACT WELDING [18] for all models, with the welding parameters outlined in Table 1, by performing coupled thermo-mechanical analyses. A Goldak double ellipsoidal heat source model [19] was adopted, where the dimensions of the Goldak heat source were as follows: front part (af)=2.0 mm, rear part (ar)=4.0 mm, width (b)=6.0 mm, depth (d)=5.5 mm.

The thermal boundary conditions were considered to be constant, with values of the convective heat transfer coefficient (h)= 20 W/m^2*K, contact heat transfer coefficient (a)=1000 W/m^2*K and emissivity=0.6.

Temperature measurements were taken at points A and B (Fig. 6), which were located 2 mm from the weld foot on the top surface and at the centre of the bottom plate, respectively.

MECHANICAL ANALYSIS

A coupled thermo-mechanical analysis was conducted using the commercial software SIMUFACT WELDING [18], and a mechanical analysis was carried out in order to evaluate the welding angu-lar deformation and longitudinal residual stress on the fillet weld joint. The phase change was not considered in this study, since this occurs at high temperatures in the material and the residual stress effects from welding are small [20], [21]. As shown in Fig. 7, an elastic perfectly plastic ma-terial model is employed, with mechanical behavior that varies as a function of temperature, in ac-cordance with the assumed statement, the influence of the solid-state phase transformation for steel is not considered.

The angular deformation and longitudinal residual stresses were calculated at the middle of the welding line, across the width of the flange. The mechanical boundary conditions were the same as those implemented in [1], as shown in Fig. 1.

ANALYSIS RESULTS FOR THE PROPOSED CASES

This section presents the results of thermal and mechanical analyses for the various models given in Table 3.

THERMAL RESULTS

A thermal analysis was conducted to optimise the weld pool characteristics, and stable and deep penetration was achieved for both passes for case A-1 (Fig. 8). Temperature histories for points A and B in Model 1 are shown in Figs. 9 and 10. At point B, the maximum temperature values were approximately 800°C for the 6 mm plate and 500°C for the 9 mm plate, whereas at point A, a rela-tively constant temperature of 600°C was observed for both thicknesses, indicating minimal influ-ence from the plate thickness on the thermal profile at this location.

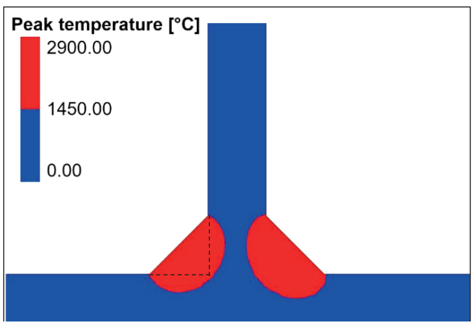

Fig. 8. Weld pool at the mid-weld line

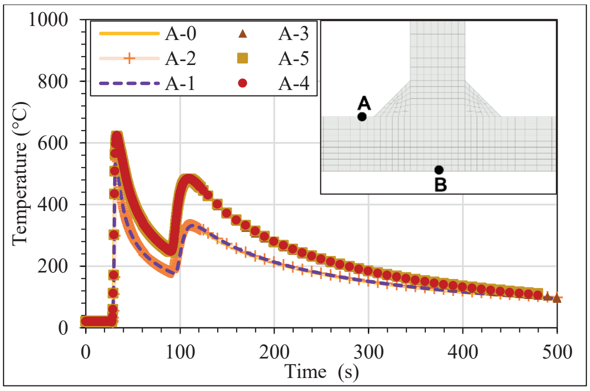

Fig. 9. Comparison of temperature profiles at point A (plate thicknesses 6 mm and 9 mm)

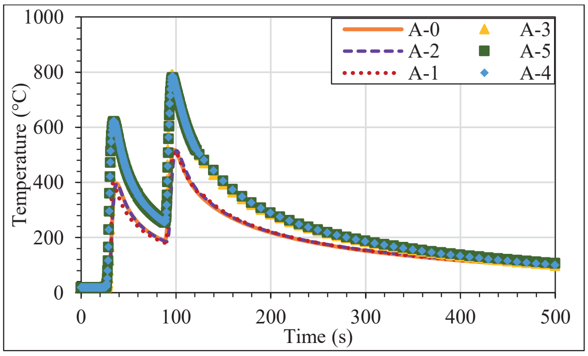

Fig. 10. Comparison of temperature profiles at point B (plate thicknesses 6 mm and 9mm)

In summary, the thermal results presented here indicate a minimal influence from the plate thick-ness on temperature at point A, with variations below 10%. However, the temperature at point B exhibits a pronounced dependence on plate thickness, with differences reaching approximately 30%; this is due to the temperature distribution through the thickness direction, which shows faster dissipation in thinner plates.

WELDING DEFORMATION RESULTS

A welding deformation analysis was also performed to assess the influence of plate thickness and web height. Fig. 11 shows the welding angular deformation, which is similar to Fig. 4, with mini-mal left-side deformation and positive right-side deformation.

The thicker plate (9 mm) exhibited significantly greater angular deformation compared to the 6 mm plate, and a 100 mm web height had 5% more angular deformation than a 300 mm web height. For the 6 mm plate, the variation in web height (100 mm vs. 300 mm) shows 15% difference in angular deformation, whereas the effect was less pronounced for the 9 mm plate. This relationship is aligned with the findings reported by Satoh [22], who established a correlation between the net heat input of the welding process and the square of the effect of flange thickness on the welding angular deformation. The angular deformation depends on the ratio Q/h^2, increasing to a maximum value before decreasing.

From an analysis of the results for the 6 mm and 9 mm plate thicknesses, it was determined that the 9 mm plate had an energy/volume ratio of 11 J/mm³, whereas a value of 25 J/m³ was obtained for the 6 mm plate. A higher angular deformation was obtained for the 9 mm plate thickness, due to a higher point on the angular deformation curve. Thus, depending on the heat input, thinner plates can exhibit less angular deformation than thicker plates when the same heat input is applied.

These results are similar to those of other studies [23] [24] linking angular deformation to tempera-ture gradients, which have given values of 429 K/m and 209 K/m for 9 mm and 6 mm plates, re-spectively.

The use of a wider web was also found to have a direct relationship with the structural rigidity, which impacts the angular distortion (Fig. 11). However, increasing the web width did not signifi-cantly influence the behaviour of the residual stresses, as can be observed from Figs. 14 and 15. Since the variation in heat input is thickness-dependent, it will have a more pronounced effect on the magnitudes and distributions of the residual stresses.

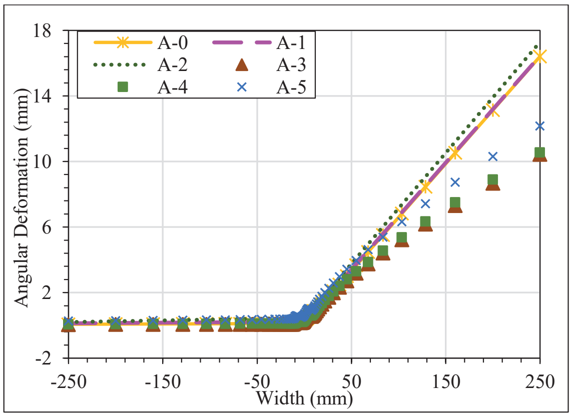

Fig. 11. Angular distortion profile at the weld centre

LONGITUDINAL WELDING RESIDUAL STRESS RESULTS

Tensile residual stress is one type of imperfection generated by the welding process [25], [26], and is well-documented as reducing the fatigue life of welded joints [27], [28] by promoting crack ini-tiation and propagation[24], [29].

Figs. 11 and 12 enable a comparison of the longitudinal residual stress profiles across the mid-weld position for plate thicknesses of 6 mm and 9 mm. Minimal variation in longitudinal residual stress is observed, indicating negligible influence of the plate thickness within the investigated range. This behaviour is aligned with the findings of previous research suggesting that longitudinal resid-ual stresses are primarily influenced by thermal input, which was consistent in both models [30].

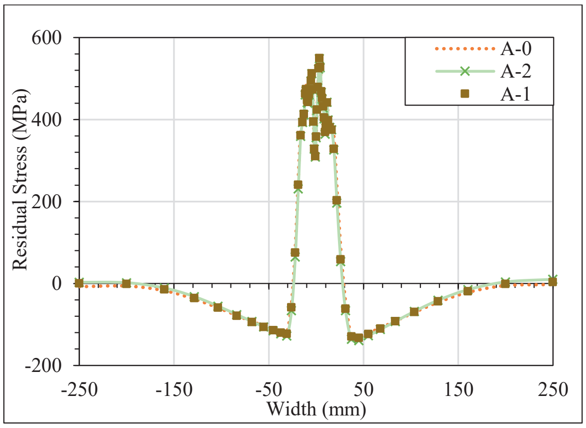

Fig. 12. Longitudinal residual stress at the weld mid-pass (9 mm plate)

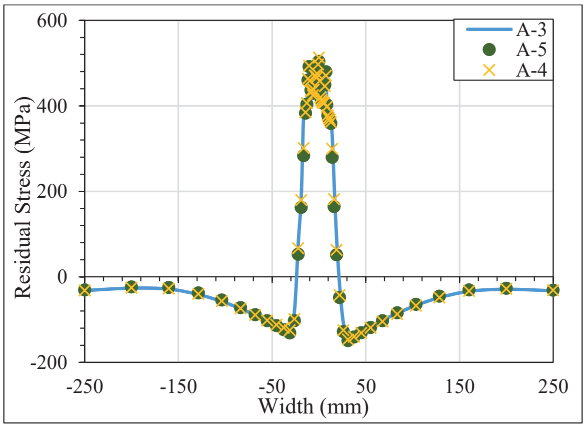

Fig. 13. Longitudinal residual stress at the weld mid-pass (6 mm plate)

WELDING DEFORMATION DUE TO DIFFERENT PLATE WIDTH

In this section, the effect of plate width on welding deformation is examined by analysing a thick plate with varying web heights.

Fig. 14 presents the deformation profiles for a plate of 9 mm thickness with two different web heights measured across the mid-weld line. The results indicate a negligible impact of both web height and plate width on welding deformation within the parameter ranges studied here.

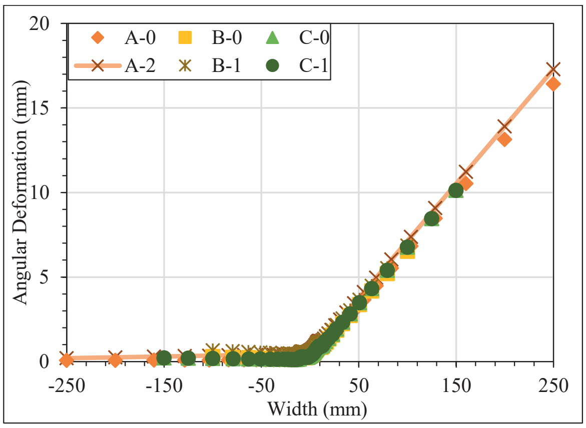

Fig. 14. Effect of welding on deformation for a 9 mm plate

Fig. 15 compares the welding angular deformation profiles for a plate 6 mm thick with varying web heights. While the overall angular deformation magnitude remained consistent, a 15% increase in maximum deformation was observed for the 6 mm plate with a 100 mm web height compared to the larger web height configuration. This finding supports the trend identified from Fig. 11, where a reduced web height was correlated with increased angular deformation.

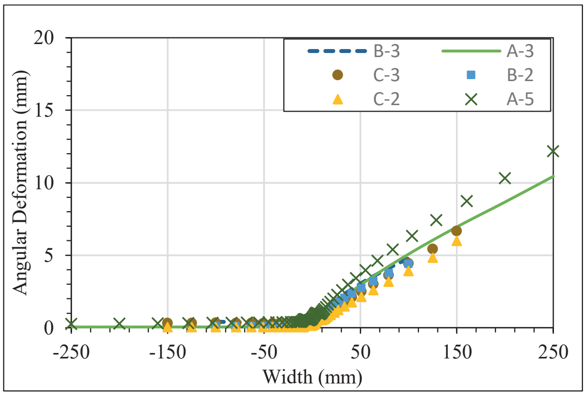

Fig. 15. Effect of welding on deformation for a 6 mm plate

CONCLUSION

This study has successfully validated the ability of a welding process simulation to accurately pre-dict the welding deformation and residual stresses in fillet-welded joint geometries.

1. By employing an FEA approach, the influence of the plate dimensions on these phenomena was quantified.
2. A direct correlation between web height and deformation was observed. Specimens with the lowest web height exhibited an increment in angular deformation of up to 15% com-pared to the average value across all web heights.
3. The results indicated that plates 9 mm in thickness experienced greater deformation com-pared to 6 mm plates, despite the identical heat input. This phenomenon is attributed to the angular deformation depending on the ratio Q/h2, which increases to a maximum before de-creasing. Thus, depending on the heat input, thinner plates may exhibit less angular defor-mation than thicker plates when the same heat input is applied.
4. While no statistically significant influence of the web height on the magnitude of the over-all residual stress was found, the area of tensile residual stresses was observed to be larger in the 9 mm plates compared to the 6 mm plates. This minimal difference may be attributa-ble to the relatively small variation in plate thickness considered in this study.
5. These conclusions can be generalised under study conditions similar to those considered here; however, when referring to different joint configurations or welding techniques, it is recommended to perform specific simulations or tests.

ACKNOWLEDGEMENTS

This study was made possible thanks to funds granted by the National Secretariat of Science, Technology and Innovation (SENACYT), through the Public Call for the Promotion of R&D (FID) 2023, under project FID23-051.

REFERENCES

1. A. Bhatti, Z. Barsoum, H. Murakawa, and I. Barsoum, "Influence of thermo-mechanical material properties of different steel grades on welding residual stresses and angular distortion," Materials and Design, vol. 65, pp. 878–889, Jan. 2014, doi: 10.1016/j.matdes.2014.10.019.
2. G. Fu, M. I. Lourenco, M. Duan, and S. F. Estefen, "Effect of boundary conditions on residual stress and dis-tortion in T-joint welds," J Constr Steel Res, vol. 102, pp. 121–135, 2014, doi: 10.1016/j.jcsr.2014.07.008.
3. R. M. F. Paulo, F. Teixeira-Dias, and R. A. F. Valente, "Numerical simulation of aluminium stiffened panels subjected to axial compression: Sensitivity analyses to initial geometrical imperfec-tions and material proper-ties," Thin-Walled Structures, vol. 62, pp. 65–74, 2013, doi: https://doi.org/10.1016/j.tws.2012.07.024.
4. L. Wei and D. Deng, "Influences of heat input, welding sequence and external restraint on twist-ing distortion in an asymmetrical curved stiffened panel," Advances in Engineering Software, vol. 115, pp. 439–451, Jan. 2018, doi: https://doi.org/10.1016/j.advengsoft.2017.11.002.
5. W. Liang, X. Hu, Y. Zheng, and D. Deng, "Determining inherent deformations of HSLA steel T-joint under structural constraint by means of thermal elastic plastic FEM," Thin-Walled Structures, vol. 147, Feb. 2020, doi: 10.1016/j.tws.2019.106568.
6. T. Urbański, A. Banaszek, and W. Jurczak, "Prediction of Welding-Induced Distortion of Fixed Plate Edge Using Design of Experiment Approach," Polish Maritime Research, vol. 27, no. 1, pp. 134–142, Mar. 2020, doi: 10.2478/pomr-2020-0014.
7. D. L. Chandramohan, K. Roy, H. Taheri, M. Karpenko, Z. Fang, and J. B. P. Lim, "A State of the Art Review of Fillet Welded Joints," Materials, vol. 15, no. 24, pp. 1–31, Dec. 2022, doi: 10.3390/ma15248743.
8. M. S. Zhao, C. K. Lee, T. C. Fung, and S. P. Chiew, "Impact of welding on the strength of high performance steel T-stub joints," Journal of Constructional Steel Research, vol. 131, pp. 110–121, Apr. 2017, doi: 10.1016/j.jcsr.2016.12.023.
9. B. de Meester, "The weldability of modern structural TMCP steels," ISIJ International, vol. 37, pp. 537–551, 1997, doi: https://doi.org/10.2355/isijinternational.37.537.

10. R. Kamal Kassab, H. Champliaud, N. Van Lê, J. Lanteigne, and M. Thomas, "Experimental and Finite Ele-ment Analysis of a T-Joint Welding," Journal of Mechanics Engineering and Automation, vol. 2, pp. 411-421, 2012. doi: https://doi.org/10.17265/2159-5275/2012.07.002.

11. G. Fu, M. I. Lourenço, M. Duan, and S. F. Estefen, "Influence of the welding sequence on re-sidual stress and distortion of fillet welded structures," Marine Structures, vol. 46, pp. 30–55, Mar. 2016, doi: 10.1016/j.marstruc.2015.12.001.

12. Z. Li, G. Feng, D. Deng, and Y. Luo, "Investigating Welding Distortion of Thin-Plate Stiffened Panel Steel Structures by Means of Thermal Elastic Plastic Finite Element Method," Journal of Mate-rials Engineering and Performance, vol. 30, no. 5, pp. 3677–3690, May 2021, doi: 10.1007/s11665-021-05646-y.

13. Y. Martínez and R. Collazo, "Review of the effects of welding parameters on residual stresses of the process," Engineering Research Report, vol. 16, pp. 85–98, 2018, doi: https://hdl.handle.net/20.500.12806/2475.

14. J. Kozak, "Prediction of Weld Deformations by Numerical Methods-Review," Polish Maritime Research, vol. 29, no. 1, pp. 97–107, Mar. 2022, doi: 10.2478/pomr-2022-0010.

15. G. Di Bella, M. Chairi, A. Denaro, and A. Bado, "Effect of Surface Treatment on Tensile Strength of Steel Single Lap Joints Bonded with Double-Sided Acrylic Foam Tapes for Naval Appli-cations," Metals (Basel), vol. 14, no. 9, Sep. 2024, doi: 10.3390/met14091071.

16. C. Borsellino, F. Favaloro, and G. Di Bella, "Durability of Single Lap Friction Stir Welded Joints between S355-J0 Steel and AA5083 Aluminum Alloy–Mechanical Tests," Metals (Basel), vol. 14, no. 2, Feb. 2024, doi: 10.3390/met14020137.

17. Hexagon AB, "MSC Patran ," 2024.

18. Hexagon AB, "Simufact Welding ," 2024.

19. J. Goldak, A. Chakravarti, and M. Bibby, "A New Finite Element Model For Welding Heat Sources," Metal-lurgical Transactions B, vol. 15, pp. 299–305, 1984, doi: https://doi.org/10.1007/BF02667333.

20. H. Ruiz, N. Osawa, L. De Gracia, and S. Rashed, "Study on the Stability of Compressive Resid-ual Stress In-duced by High Frequency Mechanical Impact under Cyclic Loadings with Spike Loads," Weld World, vol. 64, pp. 1855–1865, 2020, doi: https://doi.org/10.1007/s40194-020-00965-5.

21. P. Michaleris, "Minimization of Welding Distortion and Buckling," in Minimization of Welding Distortion and Buckling: Modelling and Implementation, Woodhead Publising Limited, 2011, pp. 3–289. doi: 10.1533/9780857092908.1.3.

22. K. Satoh and T. Terasaki, "Effect of Welding Conditions on Residual Stresses Distributions and Welding De-formation in Welded Structures Materials," Quarterly Journal of Japan Welding Society , vol. 45, pp. 150–156, 1976, doi: ISOPE-I-02-443.

23. G. Marquis and Z. Barsoum, "A Guideline for Fatigue Strength Improvement of High Strength Steel Welded Structures Using High Frequency Mechanical Impact Treatment," Procedia Eng, vol. 66, pp. 98–107, 2013, doi: https://doi.org/10.1016/j.proeng.2013.12.066.

24. K. Anami, C. Miki, H. Tani, and H. Yamamoto, "Improving Fatigue Strength of Welded Joints by Hammer Peening and TIG-Dressing," Structural Engineering, vol. 17, no. 1, pp. 57–68, Apr. 2000, doi: https://doi.org/10.2208/jscej.2000.647_67.

25. G. Marquis, E. Mikkola, H. Yildirim, and Z. Barsoum, "Fatigue strength improvement of steel structures by high-frequency mechanical impact: proposed fatigue assessment guidelines," Welding in the world, vol. 57, pp. 803–822, 2013, doi: http://dx.doi.org/10.1007/s40194-013-0075-x.

26. H. C. Yildirim and G. Marquis, "Fatigue strength improvement factors for high strength steel welded joints treated by high frequency mechanical impact," International Journal of Fatigue , vol. 44, pp. 168–176, 2012, doi: https://doi.org/10.1016/j.ijfatigue.2012.05.002.

27. M. Tai and C. Miki, "Fatigue strength improvement by hammer peening treatment - Verification from plastic deformation, residual stress, and fatigue crack propagation rate," Welding in the world, vol. 58, pp. 307–318, 2014, doi: https://doi.org/10.1007/s40194-014-0115-1.

28. H. C. Yildirim, G. Marquis, and Z. Barsoum, "Fatigue assessment of high frequency mechanical impact (HFMI)-improved fillet welds by local approaches," International Journal of Fatigue, vol. 52, pp. 57–67, 2013, doi: https://doi.org/10.1016/j.ijfatigue.2013.02.014.

29. C. Tsai, M. Tsai, and R. B. McCauley, "Stress Analysis and Design of Double Fillet-Welded T-Joints" Welding Research Supplement, vol. 77, no. 2, pp. 94–102, Feb. 1998.

30. D. Deng, W. Liang, and H. Murakawa, "Determination of welding deformation in fillet-welded joint by means of numerical simulation and comparison with experimental measurements," Journal of Materials Processing Technology, vol. 183, no. 2–3, pp. 219–225, Mar. 2007, doi: 10.1016/j.jmatprotec.2006.10.013.